Composite Materials
2025, Vol. 9, No. 2, pp. 81–97
https://doi.org/10.11648/j.cm.20250902.13

Review Article

Physical, Mechanical, and Thermal Characterization of a Cocos Nucifera Rachis Reinforced Polyester Matrix Composite

Gallus Eric Atangana[1, 2, 5, *], Theodore Tchotang[1, 2], Joseph Nkongho Anyi[4], Zacharie Merlin Ayissi[3], Moukam Tchawe Tchawe[6]

[1]Department of Industrial and Mechanical Engineering, National Advanced School on Engineering, Yaoundé, Cameroun

[2]Department of Marine Mechanical Engineering, National Higher School of Maritime and Oceanic Sciences and Techniques (ENSTMO) of the University of Ebolowa, Kribi, Cameroon

[3]Department of Automotive and Mechatronic Engineering, National Polytechnic School of University of Douala, Douala, Cameroon

[4]Department of Mechanical Engineering, Higher Technical Teacher's Training College (HTTTC) of the University of Buea, Kumba, Cameroun

[5]Department of Mechanical Engineering, Lasalle Technical Institute of Higher Education, Douala, Cameroon

[6]Department of Mechanical Engineering, ENSAIcom University, Ngaoundéré, Cameroun

Abstract

The valorisation of natural waste proves highly promising given its abundance in our environment. In this context, we developed a polyester matrix composite reinforced with treated fibres extracted from the coconut rachis (Cocos nucifera). Prior to incorporation, the fibres were subjected to an alkaline treatment and then added at different volume fractions (10%, 15%, 20%, 25%, and 30%) into the matrix using a manual hand lay-up technique. After fabrication of the composite material, the physical, mechanical, and thermal properties of each specimen were evaluated. Regarding the physical properties, the results indicate an increase in composite porosity, ranging from 6.877% to 13.437% depending on the fibre content. The water absorption rate shows a slight, monotonic rise, averaging 0.49%. Concerning the mechanical properties, the composite containing 25% fibres exhibits the best tensile and flexural strengths, with values of 19.450 MPa and 28.718 MPa, respectively. Thermal assessment using an asymmetric hot plate device reveals that fibre incorporation enhances the thermal insulation of the material. Furthermore, X-ray diffraction (XRD) analysis highlights a predominantly amorphous structure at 0% fibre content, with characteristic peaks of polyester. From 15% onwards, crystallinity peaks associated with cellulose and minerals begin to appear. At 25% and 30%, crystallinity becomes more pronounced, reflecting improved structuring of the fibrous phases and stronger interaction with the matrix. These observations are consistent with the literature on natural fibre composites.

Keywords

Polyester Composite, Coconut Rachis Fibres, Alkaline Treatment, Mechanical and Thermal Properties, X-ray Diffraction (XRD)

*Corresponding author: gallusericatangana@yahoo.fr (Gallus Eric Atangana)

Received: 5 October 2025; **Accepted:** 3 November 2025; **Published:** 24 December 2025

1. Introduction

The use of bio-based composite materials has attracted increasing attention due to environmental concerns, as well as the pursuit of more sustainable solutions across various industrial sectors. [1, 2]. Among these materials, natural fibre-based composites, particularly those reinforced with plant fibres, offer significant advantages in terms of lightness, reduced cost, and lower environmental impact compared with composites reinforced with synthetic fibres [3]. These materials play a key role in the transition towards a circular economy and sustainable development [4]. This is particularly true in developing countries, where the valorisation of local natural resources is essential. Cameroon, rich in biodiversity and biomass, holds significant potential for the production of bio-based composites [5, 6]. Among the available resources, coconut rachis fibres (Cocos nucifera) are often regarded as agricultural by-products. Increasingly, however, they are being explored for use as reinforcement in polymer matrices. Nevertheless, the effectiveness of these natural fibres in composites largely depends on their prior treatment. This treatment aims to improve their compatibility with the matrix and to enhance their various properties. In this context, the chemical treatment of natural fibres, particularly the use of alkaline solutions such as sodium hydroxide (NaOH), is a widely applied method to modify the surface characteristics of the fibres. It also serves to reduce their lignin and hemicellulose content, thereby increasing their adhesion to the polymer matrix [7-9]. Some work has been carried out in the same direction (the work of B. Y. R. Surnam and G. Imrith, 2023 for example), but shows limits that we consider considerable for serene use (low fiber load, i.e. 0.5 to 1.5% by mass; or even the field of application). The study is limited to composites containing only 0.5% fibre loading (by weight) to determine the optimal treatment, followed by tests on single- or multi-layer arrangements with up to 1.5% loading. These percentages are very low compared to other studies (e.g. up to 30% or more) [10]. Limitation: the effect of a higher fibre percentage remains unknown. The study omits crucial analyses such as long-term behaviour, moisture influence, and ageing. Yet, natural fibres are often hydrophilic, which may compromise the durability of the composite (general reference on biocomposites) [11, 12]. The study suggests potential applications for non-structural products (tiles, decorative edges), implying that these composites are unsuitable for structural or high mechanical stress applications [13].

In this study, coconut rachis fibres derived from Cameroonian biomass were treated with a 3% NaOH solution for 120 hours. The objective was to enhance their physical, mechanical, and thermal properties. Subsequently, a polyester matrix composite reinforced with these fibres was developed. The expected results will highlight the potential of these treated fibres as reinforcement for the production of high-performance and durable composites. They will also provide insights into their ability to meet the requirements of industrial applications, while contributing to the valorisation of local resources.

2. Methodology

2.1. Materials and Experimental Procedure

The polyester resin and the treated coconut rachis fibres obtained from plantations in Cameroon are the constituents used in this work.

2.1.1. Polyester Resin

The matrix used for the development of the different biocomposites is a polyester resin. This choice is justified by the fact that this resin is relatively inexpensive and well suited to composites intended for large-scale applications. It is a synthetic product mainly employed in the manufacture of composite materials whose mechanical performance requirements are not very high (Table 1) [14]. In addition to this matrix, reinforcements may consist of synthetic materials, such as long glass fibres (in unidirectional or woven form) or short fibres (mat), as well as natural fibres of plant or animal origin.

Table 1. *Physical and Mechanical Properties of Resins [15].*

ε_r in tensile (%)	ρ (Kg/m^3)	σ_r in tensile (MPa)	E in tensile (GPa)
2 - 5	1200	50 - 80	2.8 – 3.5

2.1.2. Fibres

The fibres were extracted from the rachis of the coconut palm, scientifically known as *Cocos nucifera* (Figure 1). This species was chosen due to its abundance, as it is extensively cultivated in plantations in the South Region of Cameroon, specifically in the Océan Department. Its fruits are commercially exploited and processed in the agri-food, medical, and cosmetic sectors. The climate of Kribi is equatorial, characterised by a fairly constant temperature (around 26 ℃) and very high rainfall, particularly during the rainy season (from June to October). This climate is favourable for the growth and development of coconut palms. After harvesting, the

rachis was obtained by removing and cleaning the coconut leaves (Figure 1a). The rachis was then cut into pieces of 30–40 mm in length (Figure 1b). These pieces were peeled (Figure 1c) and subsequently immersed in water at room temperature for three months. Over time, the aqueous solvent gradually disrupted the natural binding material within the rachis structure. After 90 days of immersion, the fibres were manually extracted. Each extracted fibre was then washed and dried at 25 ℃ for one week (Figure 1d). The different fibre samples were obtained through water retting. The coconut rachis fibres were treated by immersion in a sodium hydroxide (NaOH) solution at 3% concentration for 120 hours at room temperature. This alkaline treatment, known as mercerisation, aims to remove amorphous constituents such as lignin, hemicellulose, waxes, and surface impurities. This process enhances the exposure of cellulose, increases the surface roughness of the fibres, and promotes better fibre–matrix adhesion within the composite. It also contributes to improving the crystallinity of cellulose, resulting in greater mechanical strength and enhanced thermal stability.

Figure 1. *Steps of the Coconut Rachis Fibre Extraction Process. [16].*

The physical, mechanical, and chemical characteristics are given in Table 2 below.

Table 2. *Physical, Mechanical, and Chemical Properties of Fibres Treated with 3% NaOH for 120 Hours. [16].*

FIBRES	D_{Ave} (mm)	MI_{Ave} (Tex)	RH_{Ave} (%)	TA_{Ave} (%)	P_{Ave} (g/cm^3)	Rm (Mpa)	Emoy (Mpa)	ε (%)	Lignin (%)	Hemicellulose (%)	Cellulose (%)
FRC3/120	0.203	71.44	3.57	218.9	0.939	779.766	15144.303	6.888	21,66	29,10	49,04

2.2. Composite Material Fabrication

The developed biocomposite (coconut palm rachis fibre / is polyester) contains fibre reinforcement fractions of 0, 10%, 15%, 20%, 25%, and 30% by weight. The biocomposite was manufactured as a fibre lay-up using a vacuum moulding technique, specifically the ‘bag’ method. The samples were produced as rectangular plates with dimensions: 250 × 150 × 5 mm for tensile tests, 150 × 150 × 5 mm for bending tests, and 250 × 150 × 15 mm for thermal tests, as shown in Figure 2. Each plate was then cut into five equal pieces for specific use in the respective type of test.

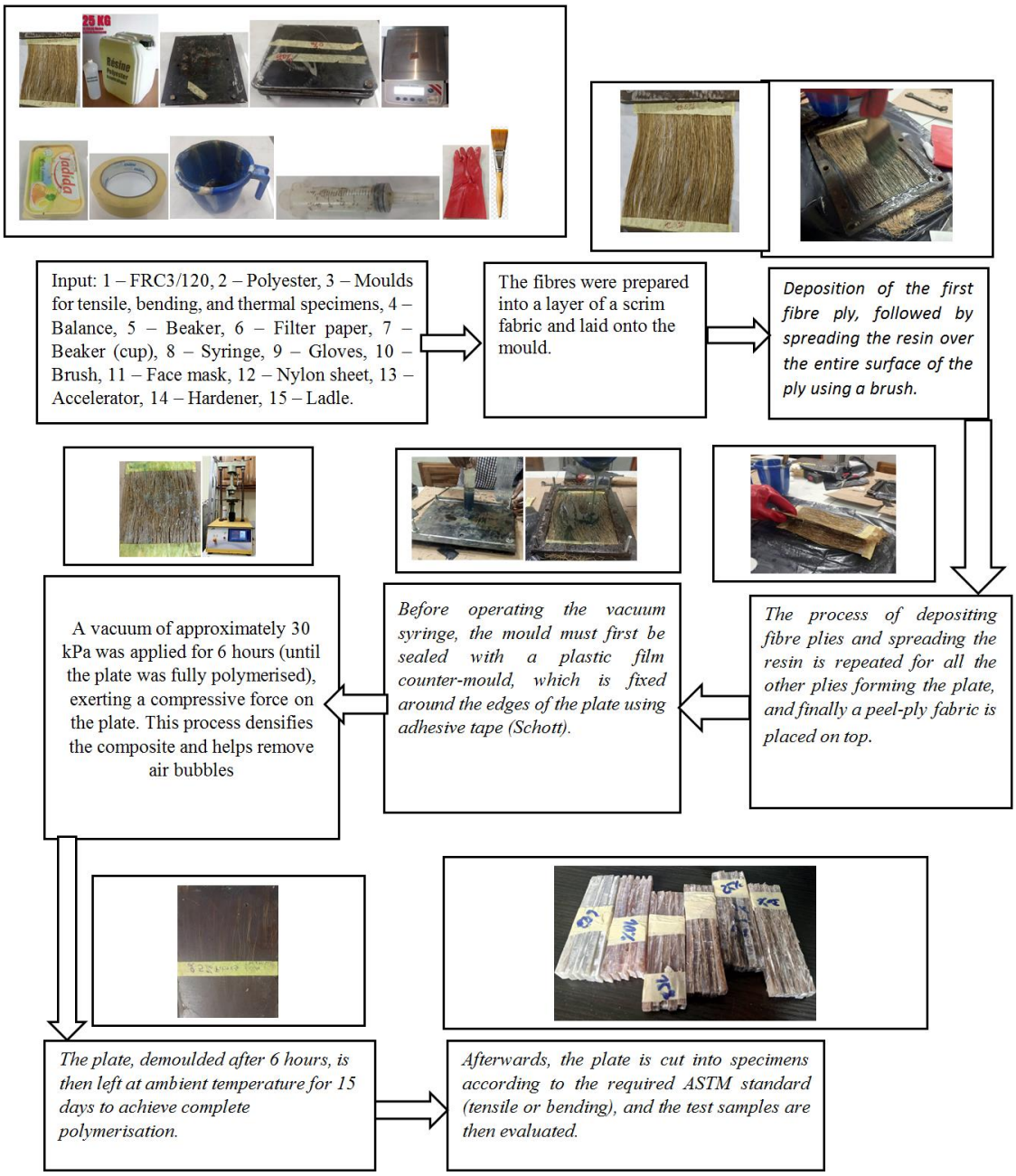

Figure 2. *Key steps in the fabrication process of the composite material.*

2.3. Physical Characterisation of the Obtained Composite Materials

2.3.1. Apparent Density of the Composites (ISO 13061-2 Standards)

The test requires the following equipment: cubic specimens, a ventilated oven, a vernier caliper, and a precision digital balance (0.001g). The samples were labelled and then dried in a ventilated oven at 60 ℃ for 24 hours. Their masses were subsequently measured using a laboratory balance, and their dimensions (length, width, and thickness) were recorded with a vernier caliper. Finally, the apparent density of each specimen (g/cm^3) was calculated using Equations (1) and (2):

$$\rho_{app} = \frac{m}{V} \tag{1}$$

$$V = \frac{L \times l \times e}{1000} \tag{2}$$

Where:

1) ρ_{app} (g/cm^3) is the apparent density of the specimen;
2) m (g) is the mass of the specimen;
3) *V (cm^3)* is the volume of the specimen;
4) *L (mm), l (mm) and e (mm)* are respectively the length, the width, and the thickness of the specimen.

2.3.2. Absolute Density of the Composite Material (ISO 1183-1 Standard)

The test was carried out in a humidity-controlled room at 80% RH and a temperature of 26.4 ℃. The water used for the test was at 26.6 ℃ with a density of 0.9968g/cm^3. This test, aimed at determining the absolute density of the samples, requires the following equipment: cubic specimens, a precision digital balance (1mg), a 0.5mm diameter wire, a thermometer, a beaker, a hydrostatic weighing bench with 10mg precision, and distilled water. The procedure involves recording two weights: the first, (m_0), corresponds to the dry specimen in air, and the second, (m_1), corresponds to the specimen immersed in water contained in the beaker and suspended from the balance by a wire. Equation (3) was then used to calculate the absolute density of the specimen.

$$\rho = \frac{m_0}{m_0 - m_1} \times \rho_{water} \tag{3}$$

Where:

1) m_0 *(g)* is the mass of the specimen weighed in air;
2) m_1 *(g)* is the mass of the specimen weighed in water.
3) ρ_{water} (g/cm^3) is the density of water.

2.3.3. Water Absorption Rate of the Composite Material

The test requires the following equipment: cubic specimens, a ventilated oven, one or more immersion tanks, a precision digital balance (0.001g), and absorbent tissues. The samples were dried in an oven at 60 ℃ for 24 hours, then weighed on a laboratory balance to obtain the dry mass (m_s) (g) of each specimen. They were subsequently immersed in tanks containing distilled water for 24 hours. At the end of this period, the specimens were removed, surface water was gently wiped off, and they were weighed on a laboratory balance to obtain the hydrated mass (m_h) (g). The water absorption rate of the samples was then determined using Equation (4).

$$AB(\%) = \frac{m_h - m_s}{m_s} \times 100 \tag{4}$$

Where:

1) AB (%) is the water absorption rate of the specimen;
2) m_s *(g)* is the dry mass of the specimen (before immersion in water);
3) m_h (g) is the mass of the specimen taken out of distilled water after 24 hours.

2.3.4. Porosity of the Composite Material (ISO 3344 Standard)

The porosity of the samples is determined using equation (5).

$$TH(\%) = \frac{(m_i - m_f)}{m_i} \times 100 \tag{5}$$

Where:

1) TH(%)is the porosity of the specimen samples.
2) m_i: initial mass of the specimen (g);
3) m_f: final mass of the specimen (g).

2.4. Mechanical Characterisation of the Composite Material

2.4.1. Static Tensile Test on the Biocomposites

Figure 3 below shows the setup used to determine the applied force (\vec{F}) and the corresponding elongation (\delta l). In our case, the distance between the grips was approximately 150mm (in accordance with ASTM D638), and the test room temperature was maintained at 22 ℃. To characterise the material, relevant material variables were introduced. Equations (6), (7), and (8) were then used to calculate the stress, strain, and Young's modulus.

$$\sigma = \frac{F}{S} = \frac{F}{a\ x\ b} \tag{6}$$

$$\varepsilon = \frac{l - l_o}{l_o} \tag{7}$$

$$E = \frac{\sigma}{\varepsilon} \tag{8}$$

Where:

F: Force (N);

S: Cross-sectional area of the specimen (mm^2);

a et *b:* Thickness and width of the specimen, respectively (mm);

l: Value obtained from the testing machine (mm);

l0: Initial gauge length (mm);

σ: Ultimate stress (MPa);

Ɛ: Strain (%);

E: Young's modulus (GPa).

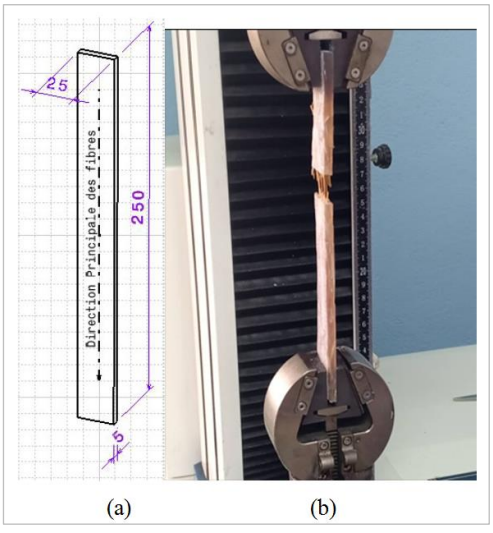

Figure 3. *Principle (a) and tensile testing (b) of the biocomposite.*

2.4.2. Three-point Bending Test on the Obtained Composites

The principle of the three-point bending test consists of placing the specimen on two supports and applying a force at a constant speed perpendicular to its surface (Figure 4). The span between the supports is approximately 70 mm (at least 16h to ensure pure bending according to ASTM D790). The test room temperature is around 22 ℃. The specimens subjected to the test are prismatic in shape with the following dimensions: h = 5 mm, L = 130 mm, b = 13 mm. The study is carried out according to ASTM D790. The mechanical properties (bending strength and flexural Young's modulus) are determined using Equations (9), (10), and (11).

$$\sigma_{f} = \frac{3\,F\,L}{2\,b\,h^2} \tag{9}$$

$$E_{f} = \frac{L^2 F}{4\,w\,b\,h^2} \tag{10}$$

$$\varepsilon_{f} = \frac{6\,w\,F}{h^2} \tag{11}$$

Where:

F: Force (N);

L: Support span (mm),

b et h: Width and thickness of the specimen, respectively (mm),

σf:: Width and thickness of the specimen, respectively (mm),

Ɛ f: Strain (%),

Ef: Flexural Young's modulus (GPa).

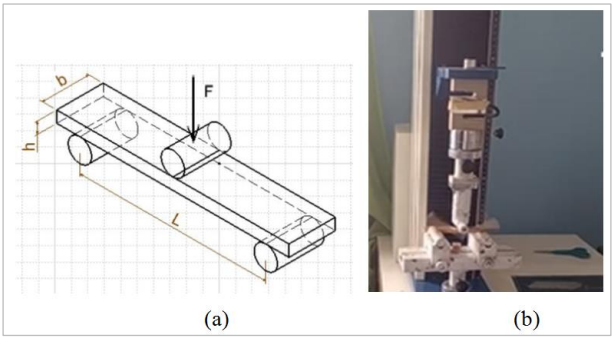

Figure 4. *Principle (a) and bending test (b) of the biocomposite.*

2.5. Thermal Characterisation of the Composite Material

The following parameters and elements are required to perform the tests: a supply voltage (U=5V), a current (I=0,504 A), the resistance of the heating ribbon or plate ($R = \frac{U}{I} = 9{,}92\Omega$), a heating surface area (S=1,5 x 10^{-3} m^2), power (P=2,52 W), and heat flux ($\varphi = \frac{P}{S} = 1680$ W/m^2), among others. The functionality of the probe must first be verified. The heating element is then mounted between two specimens, the assembly is clamped, and the voltage applied to the terminals of the stabilized power supply is set. The time and voltage values are chosen to allow a temperature rise of approximately 10 ℃, providing sensitivity to ρc. The 10 ℃ corresponds to the required temperature increase for a 1D model. Data acquisition time is set, the heat source is switched on, and data recording is performed. To initialise the program, the probe is calibrated. The thickness of the sample is measured using a vernier caliper. Once the above values are obtained, they are entered into Excel and subsequently imported into the program. The thermal properties (specific heat capacity, thermal effusivity, thermal conductivity, and thermal diffusivity) are determined using Equations (12), (13), (14) et (15):

$$C_P = \frac{1}{m} \tag{12}$$

$$E = \sqrt{\lambda . \varphi . C_P} \tag{13}$$

$$\lambda = \frac{E^2}{\rho_c\, Cp} \tag{14}$$

$$a = \frac{\lambda}{\rho_c\, Cp} \tag{15}$$

Where:

1) Cp: specific heat capacity (J kg^{-1} K^{-1})
2) m: mass of the block (kg)
3) E: thermal effusivity (J m^{-2} K^{-2} $s^{1/2}$)
4) λ: thermal conductivity (W m^{-1} K^{-1})
5) φ: heat flux (W m^{-2})
6) ρc: density (kg m^{-3})
7) a: thermal diffusivity (m^2 s^{-1})

2.6. X-ray Diffraction (XRD)

X-ray diffraction (XRD) analysis was carried out at the Coordination Chemistry Laboratory of the University of Yaounde I, Cameroon, using an ARL EQUINOX 100 diffractometer. The instrument is equipped with a copper (Cu) X-ray source and a CPS (Curved Position Sensitive) detector. The analyses were performed under an operating voltage of 40 kV and a current of 0.9 mA, within an angular range of 10–70 °(2θ), with a step size of 0.017 °(2θ) and a counting time ranging from 50 to 165 seconds per step. The device also employs a fixed divergence slit at an angle of 0.5 °, with continuous sample rotation at a rate of one revolution per second to improve signal quality. The crystallinity of the fibres within the composite was assessed using the method described in [20], which relies on the intensity of the characteristic peaks corresponding to the amorphous and crystalline phases in the diffractogram. Specifically, the peaks associated with the (101) plane (amorphous region) and the (002) plane

(crystalline region) were identified, and the maximum intensity of each peak was used to calculate the crystallinity index (CrI) according to equation (16):

$$CrI = \frac{I_{002} - I_{am}}{I_{002}} \times 100 \quad (16)$$

Where: I_{002} is the maximum intensity of the crystalline peak and I_{am} that of the amorphous peak.

Furthermore, the microfibril angle (MFA) was estimated from fibres extracted from the composite and unidirectionally aligned on a specially designed sample holder. The parameter *T*, as defined by [21], was obtained from the analysis of the 002 diffraction arc, measured around the angle 22.42 ° (2θ) within an angular range of –180 ° to 0 °, with a step size of 0.05 °. The MFA was then calculated according to Cave's equation (17):

$$MFA = 0{,}6 \times T \quad (17)$$

Where: *T* corresponds to half of the distance between the inflection points of the tangents to the intensity curve of the 002 peak.

This analysis made it possible to assess the structural organisation of the fibres within the matrix and to estimate their contribution to the overall crystallinity of the composite material.

3. Results and Discussion

3.1. Physical Characterisation of the Composite Material and the Matrix

Figure 5 below presents the results of the physical properties as a function of the fibre contents incorporated into the polyester matrix.

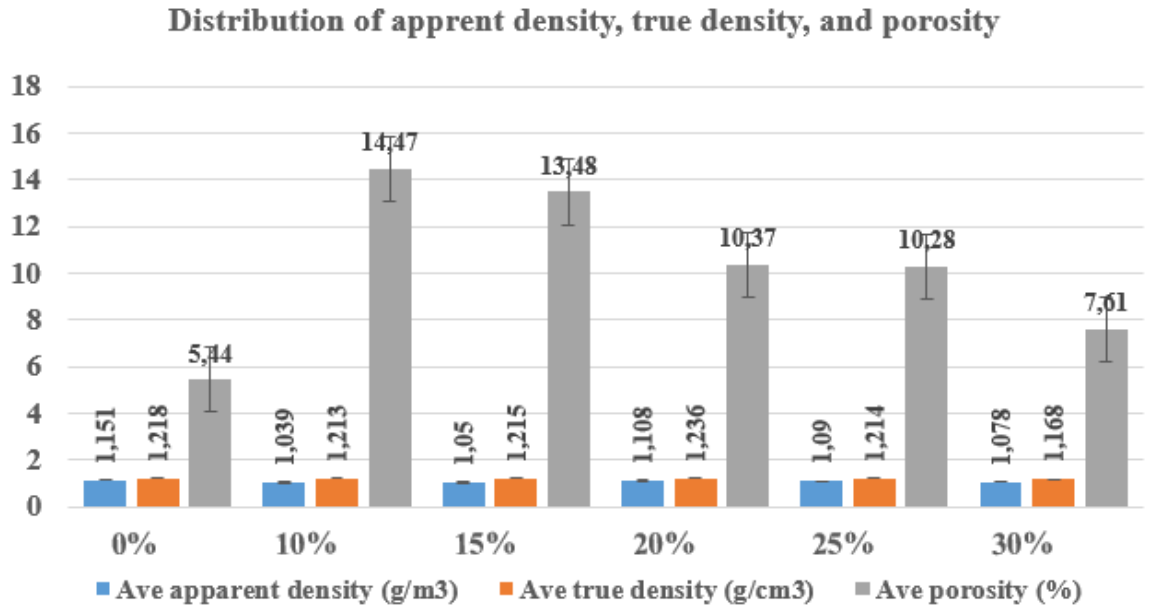

Figure 5. *Apparent density, absolute density, and porosity as a function of fibre content in the matrix.*

The alkali-treated fibres exhibit a rougher and cleaner surface than the untreated ones, as revealed by scanning electron microscopy (SEM) observations. This morphological modification promotes more effective mechanical interlocking between the matrix and the fibres. It emerges that the lowest apparent and true densities are obtained for the 30% fibre composites, with values of 1.039 g/cm^3 and 1.168 g/cm^3, respectively. Conversely, the control sample (0%) exhibited the highest apparent and true densities, namely 1.151 g/cm^3 and 1.236 g/cm^3, respectively. This decrease in density observed in the polyester composites confirms the lightweight nature of the Cocos nucifera rachis fibres [16]. It is also evident that, for all fibre contents tested, both the apparent and true densities decrease significantly with increasing fibre loading in the composites. These results are consistent with those reported by J. Sahari *et al.* [17], who investigated the effect of oil palm ash on the mechanical and thermal properties of unsaturated polyester composites, as well as by S. Mohd Yusuf *et al.* [18] who studied the physical, mechanical and thermal properties of sugar palm fibre-reinforced unsaturated polyester composites. Figure 5 also reveals an increase in porosity within the composites, ranging from 6.877% to 13.437% for fibre loadings of 0, 10, 15,

20 and 25%. This is followed by a decrease (down to 11.044%) for composites with a 30% fibre content. The voids present in the composites are attributed partly to moulding imperfections and partly to the natural structure of these fibres, which are inherently porous due to the presence of lumens in their cellular structure. In addition to these factors, the morphology of the fibres and their compatibility with the matrix may also contribute to the voids observed in the composites [19].

Figure 6 below shows the variation in water absorption with fibre content in the composites. The results indicate that the incorporation of fibres into the mixture leads to a slight increase in water uptake, which remains relatively steady across the studied fibre volume fractions. This suggests a progressive infiltration of water into the composite. Such behaviour is attributed to the intrinsic water absorption capacity of the fibres and the adverse effect of foreign matter (fibres) on the bonding efficiency of the composite constituents, as also reported by S. Mohd Yusuf *et al.* [18]. Furthermore, the presence of voids within the composites is another factor contributing to the higher water absorption rates.

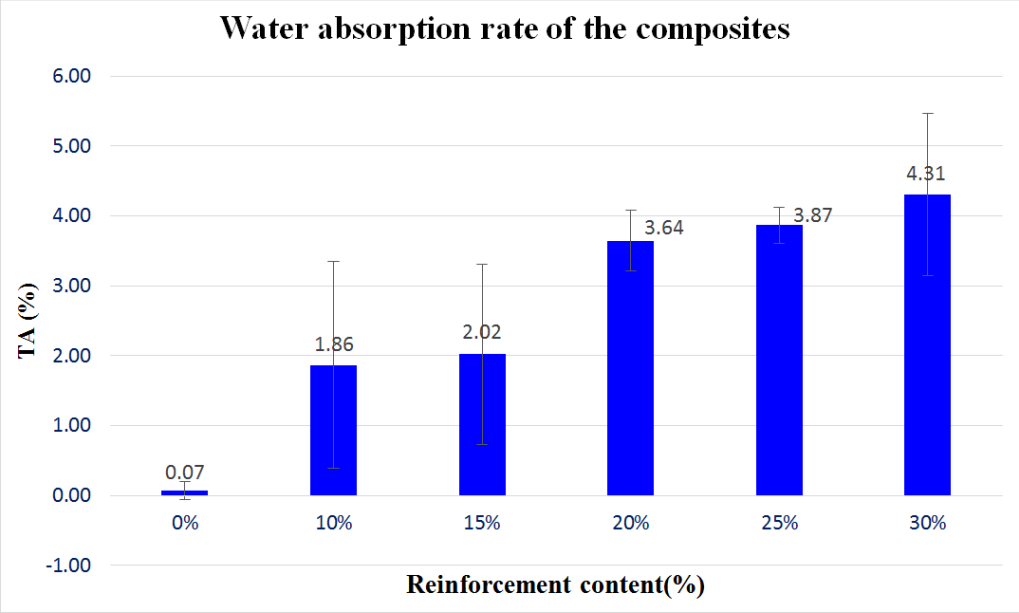

Figure 6. *Water absorption rate of the composites as a function of the fibre content in the matrix.*

The alkali treatment of *Cocos nucifera* rachis fibres improved fibre–matrix adhesion by producing rougher and cleaner fibre surfaces, enhancing mechanical interlocking within the polyester matrix. The composites showed reduced apparent and true densities with increasing fibre content, confirming their lightweight nature—an essential advantage for shipbuilding applications, where weight reduction enhances fuel efficiency and performance. Although porosity and water absorption slightly increased with fibre addition, these values remained within acceptable limits for marine environments. The stable water uptake across fibre loadings suggests good dimensional stability and adequate bonding between the fibres and matrix. Overall, the results indicate that *Cocos nucifera* rachis fibre-reinforced polyester composites offer a promising balance of low density, satisfactory mechanical integrity, and environmental sustainability. These characteristics make them suitable for use in non-structural and interior components of ships, supporting the transition toward lighter and more eco-friendly materials in the shipbuilding industry.

3.2. Mechanical Characterisation of the Composite Material and the Matrix

3.2.1. Tensile Properties of the Composites and the Matrix

Figures 7 and 8 present the results of the tensile tests performed on the polyester matrix reinforced with unidirectionally aligned coconut palm rachis fibres, for reinforcement contents of 10%, 15%, 20%, 25%, and 30%. From these figures, it can be observed that reinforcing the polyester matrix with fibrous material alters the tensile properties of the composite, as also reported in [5]. Regardless of the type of fibrous reinforcement, the incorporation of coconut palm rachis fibres into the polyester matrix induces significant changes in the mechanical properties.

It is also observed that the addition of fibres reduces the elasticity of the composite material, rendering it more rigid. The treated fibres can establish stronger interactions with the polyester matrix, resulting in good dispersion within the composite. This contributes to improved stiffness imparted by

the fibres. Another observed outcome is the initial drop in tensile strength from 17.66 MPa to 6.34 MPa when fibre content increases from 0% to 10%. Conversely, tensile strength gradually increases with higher fibre loading. The highest tensile strength is observed at 25%, which also exhibits the largest deformation (Figure 7). This behaviour can be explained by the fibre length of the rachis, as well as by decohesion between the matrix and the fibres under stress. Such decohesion generates stress concentration, accelerating sample failure. It is expected that the addition of resilient fibres increases the elongation at break. Moreover, the observed reduction in elongation at break may be attributed to decreased deformability at the rigid fibre–matrix interface, as noted in [20]. This may also result from the formation of air bubbles during specimen handling or during the mixing of fibres with the resin. The presence of these air bubbles reduces the mechanical properties, highlighting the importance of using more advanced processing techniques to ensure more reliable results [21].

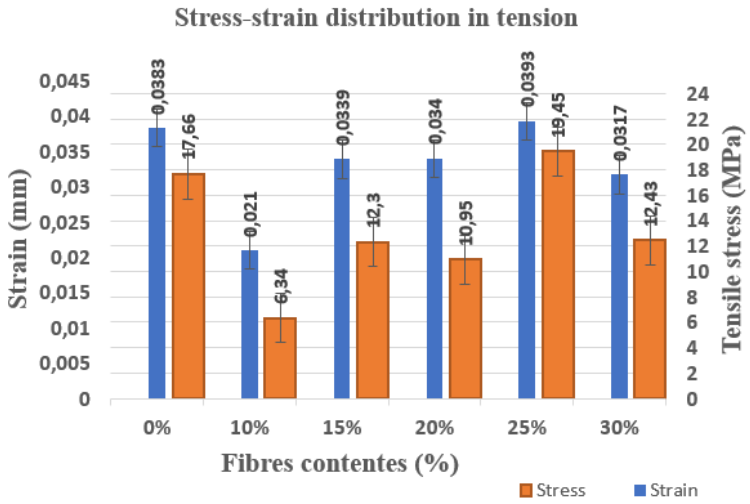

Figure 7. *Stress and strain in tension as a function of the fibre content in the matrix.*

Overall, it is noted that incorporating a small percentage of fibres initially reduces the composite's mechanical performance across all measured properties. However, progressive increases in the reinforcement fraction enable performance to match or exceed that of the neat resin, with an optimal content around 25%, as illustrated in the figure above. This can be explained by the fact that introducing a low amount of reinforcement weakens the internal structure (reduces resin compaction), particularly in composites with randomly oriented fibres, where specimen preparation can lead to the formation of air bubbles. This observation has been reported in previous studies [22]. In general, the trend indicating that mechanical properties improve with increasing reinforcement content aligns with findings widely reported in the literature [23, 24]. The results obtained here appear superior to some previously reported values in the literature *([25])*.

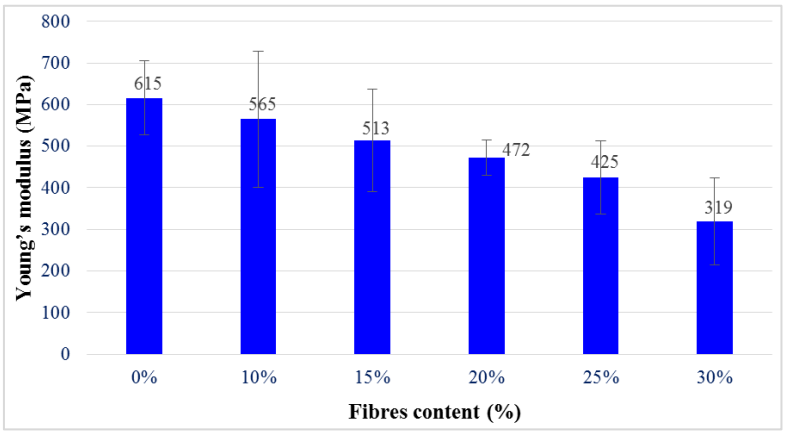

Figure 8. *Tensile Young's modulus as a function of fibre content in the matrix.*

The figure above (Figure 8) shows that increasing the fibre content from 0% to 30% by weight led to a gradual decrease in Young's modulus, from 615 MPa for the pure Polyester Resin/Coconut Rachis Fibre (PRCF) composite to 319 MPa. From a mechanical standpoint, the alkaline treatment led to a significant increase in the tensile strength and Young's modulus of the composite, confirming a more efficient stress transfer between the polyester matrix and the fibres. These improvements are attributed to the reduction of amorphous constituents (lignin and hemicellulose) and the increase in the degree of cellulose crystallinity after treatment.

The tensile results show that reinforcing polyester with *Cocos nucifera* rachis fibres enhances stiffness and tensile strength, particularly at 25% fibre content. Alkaline treatment improved fibre–matrix bonding and stress transfer, leading to better mechanical performance and structural stability. Despite an initial reduction in strength at low fibre loadings, the treated composites exhibit superior behaviour at higher reinforcement levels. Their combination of light weight, mechanical reliability, and sustainability makes them promising for non-structural shipbuilding applications.

3.2.2. Flexural Properties of the Composites and the Matrix

The results obtained from the flexural test of the polyester matrix reinforced with unidirectionally treated coconut rachis fibres at reinforcement rates of 10%, 15%, 20%, 25%, and 30% are presented in Figures 9 and 10. From these figures, it is observed that reinforcing polyester with these fibres modifies the flexural properties of the composite material, This is similar to the findings reported in the literature [26], regardless of the fibre loading ratio in the matrix. A significant increase in flexural strength is observed for fibre contents ranging from 10% to 25%. This strength decreases beyond 25%, although it does not reach the flexural strength of the pure resin (30.778 MPa). The maximum elongation is recorded for the 20% fibre-reinforced polyester composite (Figure 9), This is consistent with the results reported in [27]. In general, the optimal fibre content varies depending on factors such as the nature of the fibres and the matrix, the fibre aspect ratio, the interfacial adhesion between the matrix and the fibres, fibre agglomeration, and the treatment techniques used [28]. According to Nam et al, the optimal fibre content for coir fibres generally ranges between 17% and 25% by weight. [29] reported an optimal content of 20% for *Doum* fibres, while [30] determined a value of 25% by weight for *coconut/polyester composites*.

Based on the present results, the 25% fibre loading represents the optimal percentage for achieving the highest flexural stress in the polyester/coconut rachis fibre composite.

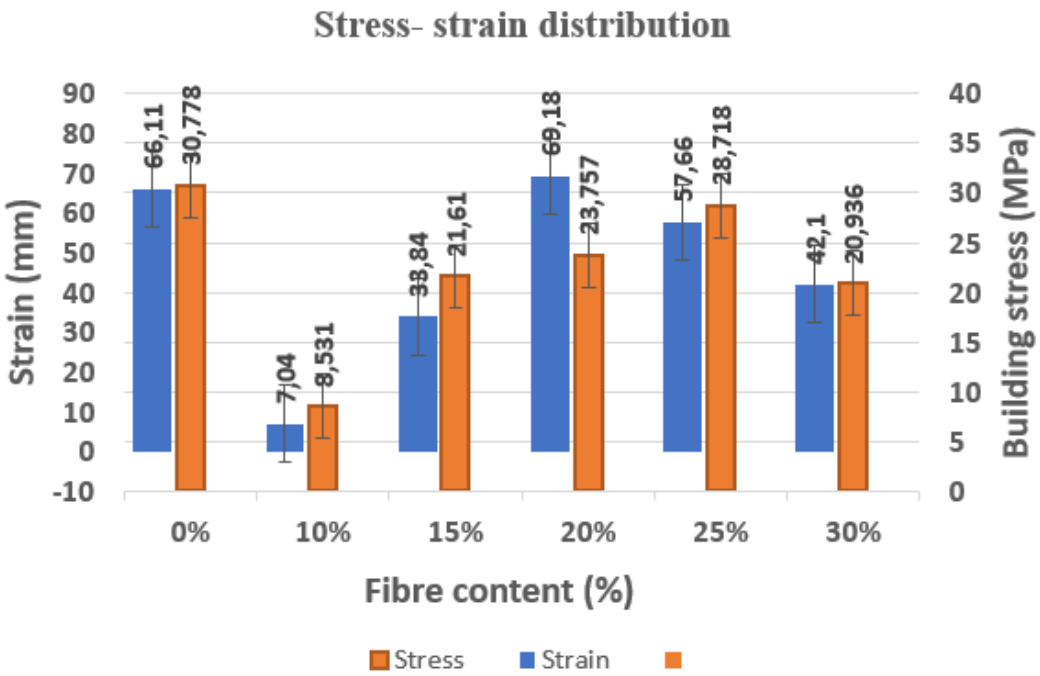

Figure 9. *Bending stress and strain as a function of the fibre content in the Matrix.*

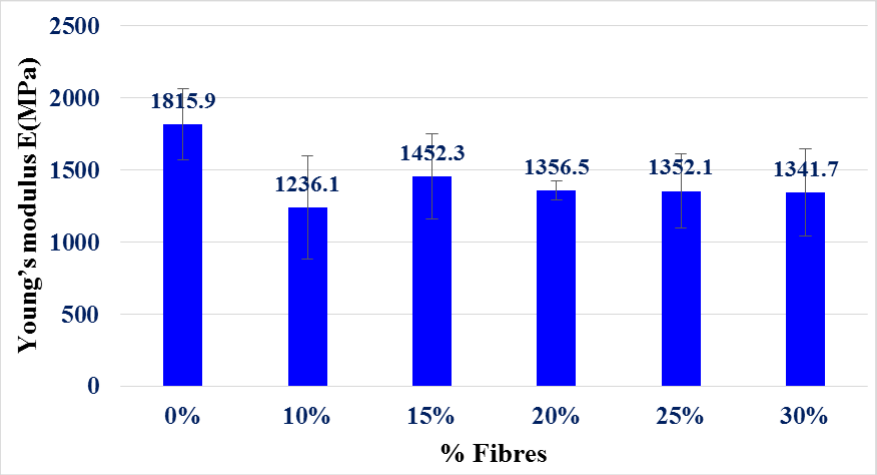

Figure 10. *Flexural modulus as a function of the fibre content in the matrix.*

We observe a decrease in the Young's modulus from 1815.9 MPa to 1236.1 MPa for 0% and 10% fibre content respectively, thereby confirming that the modulus of polyester is higher than that of the fibres within this range. Subsequently, this value increases to 1452.3 MPa at a fibre content of 15%, representing the maximum value observed among all the proportions added (Figure 10).

The polyester composite reinforced with *Cocos nucifera* rachis fibres shows strong potential for shipbuilding. Flexural strength and stiffness improved significantly, with optimal performance at 25% fibre content due to effective fibre–matrix bonding and stress transfer. Moderate fibre loadings also maintain good flexibility, balancing rigidity and resilience. Lightweight and eco-friendly, this composite is well-suited for marine applications requiring resistance to bending and dynamic loads. Its properties make it ideal for interior panels, decking, and non-structural ship components.

3.3. Thermal Characterisation of the Composite Material

Figures 11, 12, 13 and 14 show a decrease in the thermal characteristics with the addition of fibres into the polyester resin. This indicates an improvement in the thermal insulation properties of the composite material.

3.3.1. Thermal Conductivity

The thermal conductivity decreases almost linearly with the increase in fibre content within the samples, reaching its lowest value at 30% fibre loading. This behaviour can be explained by the presence of fibres in the composite, which likely created voids and made the material's structure more porous. Such a structure enhances the thermal insulation performance, as can be observed in Figure 11.

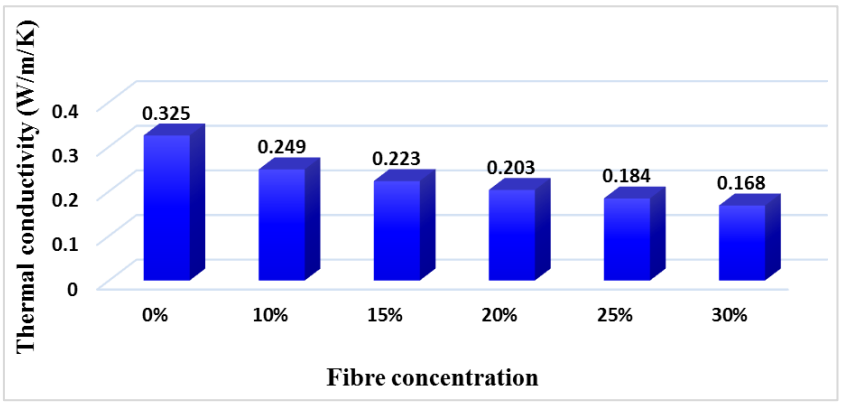

Figure 11. *Thermal conductivity as a function of the coconut rachis fibre content.*

3.3.2. Thermal Effusivity

As shown in Figure 12, the thermal effusivity of our composite decreases with the increase in fibre content. This observation has also been reported in the works of [31].

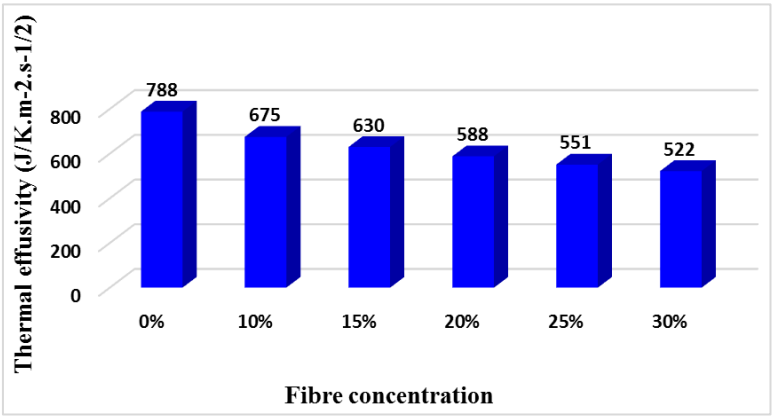

Figure 12. *Thermal effusivity as a function of coconut rachis fiber content.*

3.3.3. Thermal Diffusivity

As with the two previous parameters, the thermal diffusivity decreases with the increase in fibre content, as can be observed in Figure 13. This study highlights the very interesting insulating capacity of our composite, which falls below the preferred threshold for good thermal insulators 12E-08m^2/s according to [32]), This classifies our composite as an insulating material.

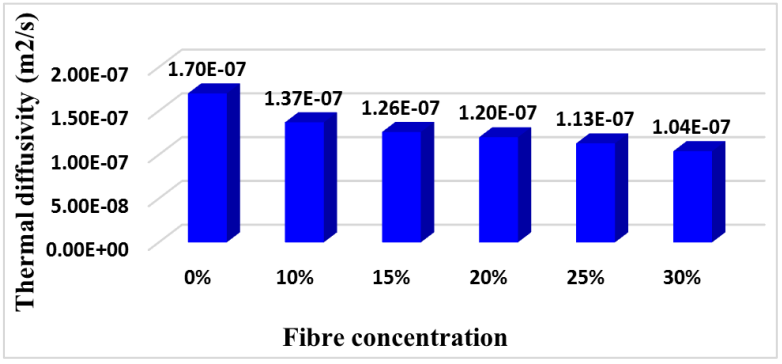

Figure 13. *Thermal diffusivity as a function of the coconut rachis fibre content.*

3.3.4. Specific Heat Capacity

The composite with a 30 wt% fibre loading exhibits a specific heat capacity value 15.18% lower than that of pure polyester, shown in Figure 14, which is *1,91E+06 J/m^3.K*. This behaviour of the composite is attributed to the lower specific heat capacity of natural fibres [33].

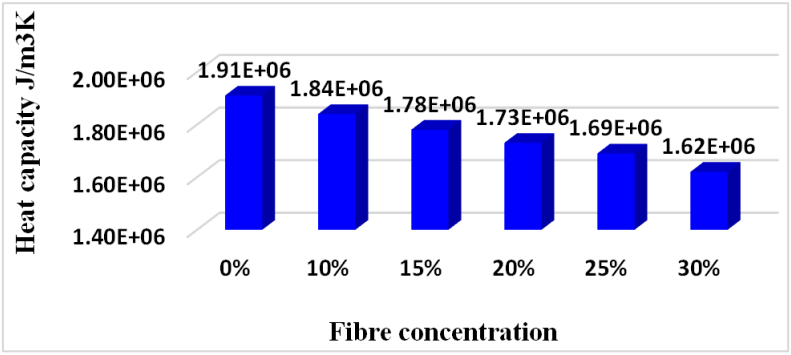

Figure 14. *Heat capacity as a function of the coconut rachis fibre content.*

From a thermal standpoint, the composite reinforced with treated fibres exhibits slightly higher stability, owing to the reduction of thermosensitive components removed during the alkaline treatment.

The thermal analysis shows that increasing *Cocos nucifera* rachis fibre content significantly reduces the composite's thermal conductivity, effusivity diffusivity and capacity, improving its insulation capacity. At 30% fibre loading, the material exhibits optimal thermal resistance due to enhanced porosity and reduced heat transfer. These properties are highly beneficial for shipbuilding, offering better temperature regulation, passenger comfort, and energy efficiency. Combined with its light weight and sustainability, the composite is ideal for insulating panels and interior marine structures.

3.4. X-ray Diffraction (XRD)

X-ray diffraction (XRD) analysis was carried out to identify the structural evolutions of the composite material as a function of the natural fibre content. A clear transition from an amorphous to a semi-crystalline state is observed as the fibre proportion increases. Table 1 presents the trends observed in the polyester matrix composite reinforced with coconut palm rachis fibres.

From Figure 15, the dominant amorphous phase (peak around ~21 °) present at all fibre contents corresponds to the amorphous structure of polyester. Its intensity slightly decreases at 30%, indicating that the fibres disrupt the regularity of the polymer matrix, as noted by [34, 35]. The mineral peaks at 27 °, 77 °, 99 °, and 111 ° are associated with silicates (α-quartz), metallic oxides (Al_2O_3, CaO), and residual mineral components originating from the fibres. Their intensity increases with the fibre content, particularly beyond 25–30%, indicating crystalline structuring induced by the treated fibres [36, 37]. The increasing complexity with fibre addition is marked by a rise from 3–4 main peaks at 10–20% to 5–6 well-defined peaks at 25–30%, revealing enhanced matrix–fibre interaction and a greater presence of crystalline components such as silicates or residual oxides [38]. Table 3 further shows that increasing the coconut rachis fibre content in the polyester matrix maintains the amorphous polyester phase up to 20%, then introduces distinct crystalline phases at 25–30%. This behaviour demonstrates a reinforced composite structure due to mineral compounds present in the fibres or their residues following alkaline treatment.

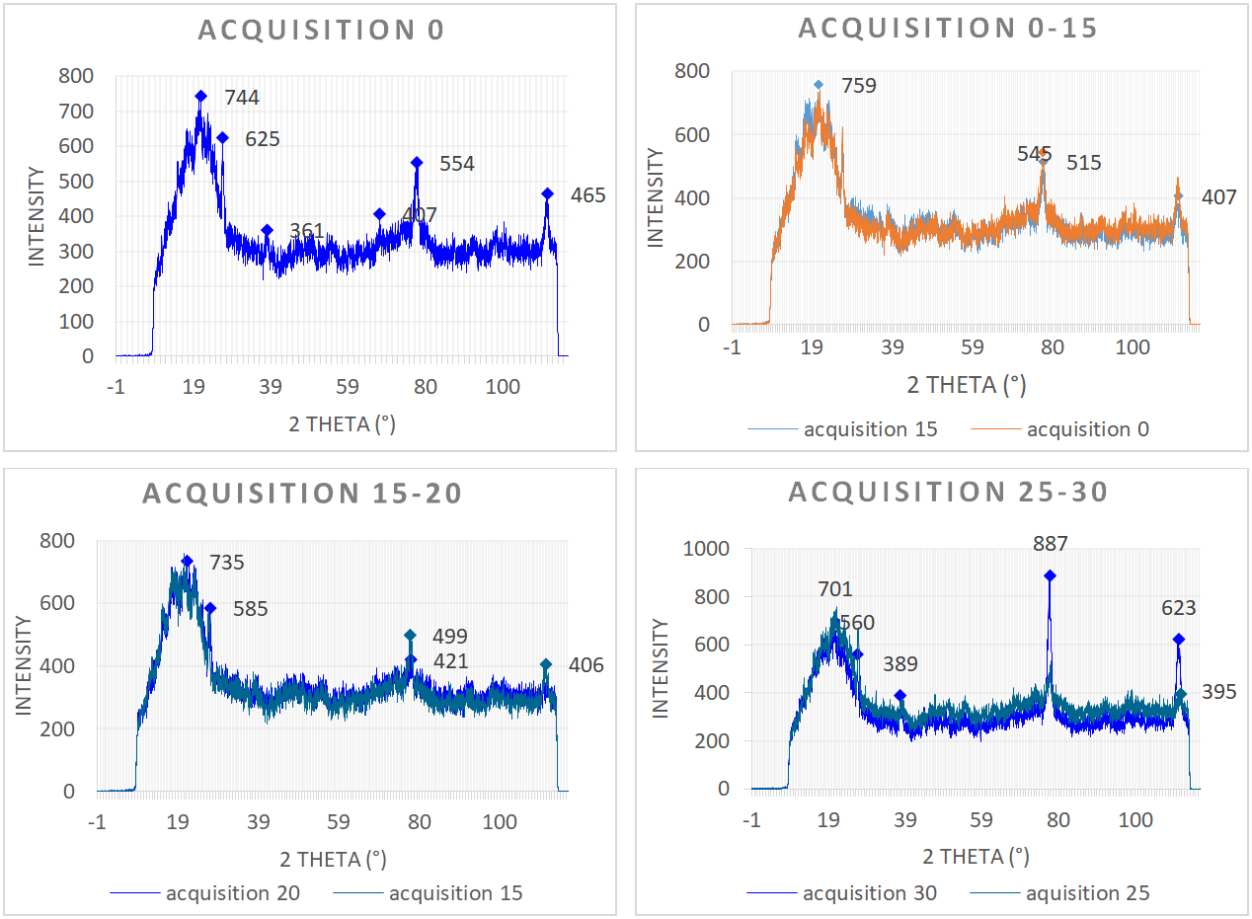

Figure 15. *X-ray diffraction curves of the composite material as a function of the coconut rachis fibre content.*

Table 3. XRD – Evolution According to Fibre Content.

% Fibres	Pics principaux (2θ)	Nature of the Peaks	Structural Behaviour	References
0%	21 °; 27 °; 38 °; 68 °; 77 °; 111 °	Amorphous Polyester + Silica (Matrix)	The structure is predominantly amorphous, with a few mineral inclusions visible within the pure polyester matrix.	[29-31]
10%	21 °; 27 °; 77 °	Polyester + Initial Fibre Additions	The mineral signature of the fibres (silica, quartz) appears while the amorphous phase of the polyester matrix is largely preserved.	[30-32]
15%	21 °; 27 °; 77 °; 99 °	Silicates and α-quartz.	Crystallinity begins to increase due to the mineral structure of the coconut fibres, although the polyester matrix remains dominant.	[31-33]
20%	21 °; 27 °; 77 °	Silica and fibre residues.	Some secondary peaks disappear, indicating overlapping or structural disorder, while the intensity of well-structured fibre-related signals increases.	[30, 32, 33]
25%	21 °; 27 °; 78 °; 99 °; 112 °	Quartz, silicates, and oxidised residues (Al_2O_3, CaO).	Progressive enrichment in crystalline minerals derived from the fibres, with the NaOH treatment promoting crystallisation.	[29, 31, 32]
30%	21 °; 27 °; 38 °; 77 °; 111 °	Quartz (77 °), silicates, and metallic oxides.	Marked crystallinity with a stabilised structure around the mineral phases, indicating enhanced fibre–matrix interaction.	[31-33]

Table 4 illustrates the behaviour of the material at each percentage interval, indicating the apparent crystallinity and the overall structural arrangement.

Table 4. Correlation with Material Structure.

Fibre Content	Apparent Crystallinity	Overall Structure
0–10%	Low	Amorphous Matrix Dominant
15–20%	Medium	Onset of Crystallinity (Fibres)
25–30%	High	Reinforcement by Fibres + Mineral Fillers

Cellulose I, the main crystalline phase of natural fibres, is clearly identified by peaks at approximately 15 °and 22 °(2θ) from 10% fibre content, with maximum intensity observed at 25% [29, 35].

From 20% fibre content, the peaks become sharp and intense, indicating improved crystalline structuring as noted by [36, 37].

Beyond 25%, dispersion issues and saturation of the polyester matrix appear, leading to increased background noise and irregularities in the XRD profiles [38, 39].

The XRD study on our composite highlighted the progressive evolution of the material's crystalline structure. While the 0% fibre sample exhibits a typical amorphous polyester nature as shown in Figure 15 at 0% acquisition fibers, increasing fibre content induces the appearance and intensification of crystalline peaks characteristic of cellulose I, particularly at ~15 °and ~22 °(2θ) (also noted by [40, 41]). Crystallinity is optimal between 20% and 25% fibre content, where the structure remains stable and well integrated. At 30%, matrix saturation causes heterogeneous dispersion and partial loss of structural order, as observed by [42]. These results confirm that a judicious addition of plant fibres enhances the internal structuring of the composite, with a potential positive impact on its mechanical and thermal properties, as highlighted by [43, 44].

4. Conclusion

The objective of this research was to develop and characterise a thermosetting composite. All composite samples were prepared as a single fibre layer using a vacuum moulding

technique. These polyester-matrix composites, reinforced with alkali-treated coconut rachis fibres (Cocos nucifera) at weight fractions of 0, 10%, 15%, 20%, 25%, and 30%, were fabricated in rectangular form. It was observed that the addition of fibres slightly increases water absorption, with a monotonic trend across the studied volume fractions. In contrast, porosity initially increases and then decreases. This progressive variation in fibre content reduces the mechanical properties, particularly the Young's modulus in tension and bending. Thermal analysis of the composites revealed a slight improvement in thermal insulation properties. Given the physical, mechanical, and thermal characteristics of the resulting material, it shows potential for applications in various industrial sectors, including shipbuilding, coke for ocean liners, wafers, the interior panels, decking, and non-structural ship components and doors.

Further investigations are required to deepen the characterisation of this composite material. Hardness tests would help evaluate its resistance to indentation and wear, while resilience tests would provide a better understanding of its energy absorption capacity under impact. An acoustic study could offer essential insights into its behaviour in sound insulation or absorption, thereby opening potential applications in the naval sector.

Moreover, a detailed chemical analysis of the composite would allow the identification of molecular-scale interactions between the matrix and the treated fibres, providing key information to optimise compatibility, enhance durability, and tailor formulations for specific operating environments.

Abbreviations

Code	Designation
XRD	X-ray Diffraction
NaOH	Sodium Hydroxide
FRC3/120	Coconut Spine Fiber of 3% NaOH Concentration for 120 Hours
e.g	Example
MPa	Mega Pascal
Ave	Average
MV	Apparent Density
APP	Absolute Density

Funding

The authors received no financial support for the research, authorship, and/or publication of this article.

Author Contributions

Gallus Eric Atangana: Conceptualization, Formal Analysis, Funding acquisition, Investigation, Methodology, Writing – original draft, Writing – review & editing

Theodore Tchotang: Methodology, Project administration, Supervision, Validation

Joseph Nkongho Anyi: Formal Analysis, Investigation, Supervision, Visualization

Zacharie Merlin Ayissi: Methodology, Visualization

Moukam Tchawe Tchawe: Formal Analysis, Investigation

Conflicts of Interest

We, the authors, declare that we have no conflicts of interest regarding the publication of this document.

References

[1] D. Carvalho et al., «Advancing Sustainability in the Automotive Industry: Biopreprегs and Fully Bio-Based Composites », Compos. Part C Open Access, p. 100459, 2024. https://doi.org/10.1016/j.jcomc.2024.100459

[2] A. Khan, S. M. Rangappa, S. Siengchin, et A. M. Asiri, Biobased Composites: Processing, Characterization, Properties, and Applications. John Wiley & Sons, 2021. https://doi.org/10.1002/9781119641803

[3] L. R. M. de Lima, A. C. Dias, T. Trindade, et J. M. Oliveira, «A comparative life cycle assessment of graphene nanoplatelets-and glass fibre-reinforced poly (propylene) composites for automotive applications », Sci. Total Environ., vol. 871, p. 162140, 2023. https://doi.org/10.1016/j.scitotenv.2023.162140

[4] A. Soni, S. Kumar, B. Majumder, H. Dam, V. Dutta, et P. K. Das, "Synergy of waste plastics and natural fibers as sustainable composites for structural applications concerning circular economy", Environ. Sci. Pollut. Res., vol. 31, no 27, p. 38846-38865, 2024. https://doi.org/10.1007/s11356-023-26365-y

[5] S. Akromah, N. Chandarana, et S. J. Eichhorn, "Mycelium composites for sustainable development in developing countries: The case for Africa", Adv. Sustain. Syst., vol. 8, no 1, p. 2300305, 2024. https://doi.org/10.1002/adsu.202300305

[6] A. Gatto, "Towards sustainable global food and biomass systems: Interactions between food loss and waste reductions, dietary shifts, and transitioning to a circular bio-based economy", PhD Thesis, Wageningen University, 2024. https://doi.org/10.18174/648608

[7] J. S. N. Raju, M. V. Depoures, et P. Kumaran, "Comprehensive characterization of raw and alkali (NaOH) treated natural fibers from Symphirema involucratum stem", Int. J. Biol. Macromol., vol. 186, p. 886-896, 2021. https://doi.org/10.1016/j.ijbiomac.2021.07.061

[8] C. M. Suárez, P. R. Montejo, et O. G. Junco, "Effects of alkaline treatments on natural fibers", in Journal of Physics: Conference Series, IOP Publishing, 2021, p. 012056. https://doi.org/10.1088/1742-6596/2046/1/012056

[9] B. Koohestani, A. Darban, P. Mokhtari, E. Yilmaz, et E. Darezereshki, "Comparison of different natural fiber treatments: a literature review", Int. J. Environ. Sci. Technol., vol. 16, p. 629-642, 2019. https://doi.org/10.1007/s13762-018-1890-9

[10] D. L. Faria et al., "Physical and mechanical properties of polyurethane thermoset matrices reinforced with green coconut fibres", J. Compos. Mater., vol. 54, no 30, p. 4841-4852, 2020. https://doi.org/10.1177/0021998320940023

[11] M. Zwawi, « A review on natural fiber bio-composites, surface modifications and applications », molecules, vol. 26, no 2, p. 404, 2021. https://doi.org/10.3390/molecules26020404

[12] F. Aramide, P. Atanda, et O. Olorunniwo, "Mechanical properties of a polyester fibre glass composite", Int. J. Compos. Mater, vol. 2, no 6, p. 147-151, 2012. https://doi.org/10.5923/j.cmaterials.20120206.06

[13] S. Sisodia, E. K. Gamstedt, F. Edgren, et J. Varna, "Effects of voids on quasi-static and tension fatigue behaviour of carbon-fibre composite laminates", J. Compos. Mater., vol. 49, no 17, p. 2137-2148, 2015. https://doi.org/10.1177/0021998314541993

[14] E. M. Ezeh, « Advances in the development of polyester resin composites: a review », World J. Eng., 2024. http://dx.doi.org/10.1108/WJE-12-2023-0517

[15] R. Venegas, A. Torres, A. M. Rueda, M. A. Morales, M. J. Arias, et A. Porras, « Development and characterization of plantain (Musa paradisiaca) flour-based biopolymer films reinforced with plantain fibers », Polymers, vol. 14, no 4, p. 748, 2022. https://doi.org/10.3390/polym14040748

[16] G. E. Atangana, T. Tchotang, A. G. Weda ̈na, Y. R. Olembe, A. Djaligue, et N. Mahonde, "Effect of Alkaline Treatment on the Physical, Chemical, and Mechanical Properties of Coconut Palm Nucifera Rachis Fibres", J. Nat. Fibers, vol. 22, no 1, p. 2449439, 2025. https://doi.org/10.1080/15440478.2024.2449439

[17] J. Sahari et M. Maleque, "Mechanical properties of oil palm shell composites", Int. J. Polym. Sci., vol. 2016, no 1, p. 7457506, 2016. http://dx.doi.org/10.1155/2016/7457506

[18] S. Mohd Yusuf, Y. Chen, R. Boardman, S. Yang, et N. Gao, "Investigation on porosity and microhardness of 316L stainless steel fabricated by selective laser melting", Metals, vol. 7, no 2, p. 64, 2017. https://doi.org/10.3390/met7020064

[19] L. Prasad, A. Saini, et V. Kumar, "Mechanical performance of jute and basalt fiber geo-grid-reinforced epoxy hybrid composite material", J. Nat. Fibers, vol. 18, no 5, p. 694-704, 2021. https://doi.org/10.1080/15440478.2019.1645789

[20] A. K. Mohanty, M. Misra, L. T. Drzal, S. E. Selke, B. R. Harte, et G. Hinrichsen, "Natural fibers, biopolymers, and biocomposites: an introduction", in Natural fibers, biopolymers, and biocomposites, CRC press, 2005, p. 17-51. https://doi.org/10.1201/9780203508206

[21] Y. Ben Mlik, M. Jaouadi, S. Rezig, F. Khoffi, M. Slah, et B. Durand, "Kenaf fibre-reinforced polyester composites: Flexural characterization and statistical analysis", J. Text. Inst., vol. 109, no 6, p. 713-722, 2018. https://doi.org/10.1080/00405000.2017.1365580

[22] S. Shibata, Y. Cao, et I. Fukumoto, "Flexural modulus of the unidirectional and random composites made from biodegradable resin and bamboo and kenaf fibres", Compos. Part Appl. Sci. Manuf., vol. 39, no 4, p. 640-646, 2008. https://doi.org/10.1016/j.compositesa.2007.10.021

[23] P. K. Kushwaha et R. Kumar, "Effect of silanes on mechanical properties of bamboo fiber-epoxy composites", J. Reinf. Plast. Compos, vol. 29, no 5, p. 718-724, 2010. https://doi.org/10.1177/0731684408100691

[24] M. Bouaziz, "Valorization of Palm Fibers for Textile and Para-textile Applications", PhD Thesis, Doctoral Thesis. Tunisia: University of Monastir, 2020.

[25] K. M. M. Rao et K. M. Rao, "Extraction and tensile properties of natural fibers: Vakka, date and bamboo", Compos. Struct., vol. 77, no 3, p. 288−295, 2007. https://doi.org/10.1016/j.compstruct.2005.07.023

[26] B. Y. R. Surnam et G. Imrith, "Investigation on the Mechanical Properties of Coconut Leaf Stalk Fibres Reinforced Composites", J. Nat. Fibers, vol. 20, no 2, p. 2198276, août 2023, https://doi.org/10.1080/15440478.2023.2198276

[27] Y. Cao, S. Shibata, et I. Fukumoto, "Mechanical properties of biodegradable composites reinforced with bagasse fibre before and after alkali treatments", Compos. Part Appl. Sci. Manuf., vol. 37, no 3, p. 423-429, 2006. https://doi.org/10.1016/j.compositesa.2005.05.045

[28] T. H. Nam, S. Ogihara, N. H. Tung, et S. Kobayashi, "Effect of alkali treatment on interfacial and mechanical properties of coir fiber reinforced poly (butylene succinate) biodegradable composites", Compos. Part B Eng., vol. 42, no 6, p. 1648-1656, 2011. https://doi.org/10.1016/j.compositesb.2011.04.001

[29] M. Brahmakumar, C. Pavithran, et R. Pillai, "Coconut fibre reinforced polyethylene composites: effect of natural waxy surface layer of the fibre on fibre/matrix interfacial bonding and strength of composites", Compos. Sci. Technol., vol. 65, no 3-4, p. 563-569, 2005. https://doi.org/10.1016/j.compscitech.2004.09.020

[30] K. Senthilkumar, N. Rajini, N. Saba, M. Chandrasekar, M. Jawaid, et S. Siengchin, "Effect of alkali treatment on mechanical and morphological properties of pineapple leaf fibre/polyester composites", J. Polym. Environ., vol. 27, p. 1191-1201, 2019. https://doi.org/10.1007/s10924-019-01418-x

[31] G. Giada, R. Caponetto, et F. Nocera, "Hygrothermal properties of raw earth materials: A literature review", Sustainability, vol. 11, no 19, p. 5342, 2019. https://doi.org/10.3390/su11195342

[32] Y. Bounour et Y. Laraba, "L'effet des materiaux ecologiques isolants et la toiture vegetalisee sur le confort thermique et la consommation energetique dans le logement promotionnel a Annaba", 2017.

[33] B. Subrahmanyam, S. G. Krishna, R. J. Kumar, et S. Devireddy, "Experimental and micromechanical thermalcharacteristics of jute fiber reinforced polyester composites", Mater. Today Proc., vol. 18, p. 350-356, 2019. https://doi.org/10.1016/j.matpr.2019.06.311

[34] A. D. French, "Idealized powder diffraction patterns for cellulose polymorphs", Cellulose, vol. 21, no 2, p. 885-896, 2014. https://doi.org/10.1007/s10570-013-0030-4

[35] A. S. Luyt et al., "Halogen-free flame-retardant compounds. Thermal decomposition and flammability behavior for alternative polyethylene grades", Polymers, vol. 11, no 9, p. 1479, 2019. https://doi.org/10.3390/polym11091479

[36] O. Oke, H. S. Naeem, A. Muhammad, et A. S. Idriss, "Science and Technology Indonesia", 2024. https://doi.org/10.26554/sti.2024.1255

[37] SAWPAN, Moyeenuddin A., PICKERING, Kim L., ET FERNYHOUGH, Alan. Effect of various chemical treatments on the fibre tructure and tensile properties of industrial hemp fibres. Composites Part A: Applied Science and Manufacturing, 2011, vol. 42, no 8, p. 888-895. https://doi.org/10.1016/j.compositesa.2011.03.008

[38] V. K. Thakur, M. K. Thakur, et M. R. Kessler, Handbook of composites from renewable materials, design and manufacturing, vol. 2. John Wiley & Sons, 2017.

[39] KAUSAR, Ayesha. Review of fundamentals and applications of polyester nanocomposites filled carbonaceous nanofillers. Journal of plastic Film & Sheeting, 2019, vol. 35, no 1, p. 22-44. https://doi.org/10.1177/8756087918783827

[40] S. Park, J. O. Baker, M. E. Himmel, P. A. Parilla, et D. K. Johnson, "Cellulose crystallinity index: measurement techniques and their impact on interpreting cellulase performance", Biotechnol. Biofuels, vol. 3, no 1, p. 10, 2010. https://doi.org/10.1186/1754-6834-3-10

[41] D. Klemm, B. Heublein, H.-P. Fink, et A. Bohn, "Cellulose: fascinating biopolymer and sustainable raw material", Angew. Chem. Int. Ed., vol. 44, no 22, p. 3358-3393, 2005. https://doi.org/10.1002/anie.200460587

[42] L. Segal, J. J. Creely, A. Martin Jr, et C. Conrad, "An empirical method for estimating the degree of crystallinity of native cellulose using the X-ray diffractometer", Text. Res. J., vol. 29, no 10, p. 786-794, 1959. https://doi.org/10.1177/004051755902901003

[43] U. K. Vaidya et K. Chawla, "Processing of fibre reinforced thermoplastic composites", Int. Mater. Rev., vol. 53, no 4, p. 185-218, 2008. https://doi.org/10.1179/174328008X325223

[44] K. G. Satyanarayana, G. G. Arizaga, et F. Wypych, "Biodegradable composites based on lignocellulosic fibers—An overview", Prog. Polym. Sci., vol. 34, no 9, p. 982-1021, 2009. https://doi.org/10.1016/j.progpolymsci.2008.12.002